


## Article

# Parametric Analysis and Numerical Optimization of Root-Cutting Shovel of Cotton Stalk Harvester Using Discrete Element Method

Hua Liu <sup>1,2</sup> , Silin Cao <sup>2,\*</sup>, Dalong Han <sup>2</sup>, Lei He <sup>2</sup>, Yuanze Li <sup>3</sup>, Jialin Cai <sup>3</sup>, Hwei Meng <sup>1,\*</sup> and Shilong Wang <sup>1</sup>

<sup>1</sup> College of Mechanical and Electrical Engineering, Shihezi University, Shihezi 832000, China; liuhua@stu.shzu.edu.cn (H.L.); l@stu.shzu.edu.cn (S.W.)

<sup>2</sup> Institute of Machinery and Equipment, Xinjiang Academy of Agricultural and Reclamation Science, Shihezi 832000, China; 20212109027@stu.shzu.edu.cn (D.H.); 20212309101@stu.shzu.edu.cn (L.H.)

<sup>3</sup> College of Mechanical and Electrical Engineering, Xinjiang Agricultural University, Urumqi 830052, China; 20212109084@stu.shzu.edu.cn (Y.L.); 20232109091@stu.shzu.edu.cn (J.C.)

\* Correspondence: caosilin@shzu.edu.cn (S.C.); mhw\_mac@shzu.edu.cn (H.M.)

**Abstract:** Aiming at solving the problems of the high cost of manual pulling, the low reliability of existing pulling devices, and the high breaking rates and high leakage rates in the process of cotton stalk reuse after removal from the field in the Xinjiang cotton area, a soil-loosening and root-cutting cotton stalk pulling and gathering machine was researched and designed; a root-cutting force model was established; the key parameters of the V-shaped root-cutting knife were calculated and optimized; and the ranges of the slide cutting angle, the cutting-edge angle, and the soil entry angle were determined. A shoveling process simulation of the V-shaped root-cutting knife and the root-soil complex was constructed, and the working mechanism of the V-shaped root-cutting knife was clarified. In order to verify the reliability and operation performance of the V-shaped root-cutting knife, the slide cutting angle, the cutting-edge angle, and the soil entry angle were used as the test factors, and a response surface test with three factors and three levels was carried out with the root-breaking force and the mean value of the cutting resistance as the test indices. The test results were analyzed by variance analysis, and the significant factors influencing the root-breaking force in descending order were the slide cutting angle, cutting-edge angle, and soil entry angle. The degrees of influence on the mean value of the cutting resistance were ordered as follows: slide cutting angle, soil entry angle, and cutting-edge angle. In order to make the V-shaped root-cutting knife achieve the optimal working state, the parameters of the test indices were optimized, and the optimal design parameters of the V-shaped root-cutting knife were set as follows: the slide cutting angle was 48.3°, the cutting-edge angle was 43.4°, and the soil entry angle was 26.2°. The field uprooting test showed that the average pass rate of root breakage was 94.8% and the average pull-out rate of cotton stalks was 93.2%. This study provides theoretical guidance for the development of a root-breaking mechanism for cotton straw harvesters.

**Keywords:** cotton stalk harvest; V-shaped root-cutting knife; discrete element method; root-soil complex; optimize and design



**Citation:** Liu, H.; Cao, S.; Han, D.; He, L.; Li, Y.; Cai, J.; Meng, H.; Wang, S. Parametric Analysis and Numerical Optimization of Root-Cutting Shovel of Cotton Stalk Harvester Using Discrete Element Method. *Agriculture* **2024**, *14*, 1451. <https://doi.org/10.3390/agriculture14091451>

Academic Editor: Simone Bergonzoli

Received: 16 July 2024

Revised: 9 August 2024

Accepted: 20 August 2024

Published: 25 August 2024



**Copyright:** © 2024 by the authors. Licensee MDPI, Basel, Switzerland. This article is an open access article distributed under the terms and conditions of the Creative Commons Attribution (CC BY) license (<https://creativecommons.org/licenses/by/4.0/>).

## 1. Introduction

For cotton, the world looks to China, and China looks to Xinjiang [1]. As an inevitable byproduct of cotton production, the annual yield of cotton stalks in Xinjiang is as high as 16.875 million tons. At present, cotton stalks in Xinjiang are mainly returned to the field [2], resulting in a waste of resources, and the stalks do not easily rot, which affects the sowing of the next crop; the cotton yield in the next year can be affected by disease [3]. Cotton stalks are not only rich in nitrogen, phosphorus, potassium, and other trace elements but also lignocellulose, phloem fiber, crude protein, and so on, and they have great potential

for comprehensive utilization [4–7]. Removing cotton stalks from the field is an important measure to deal with agricultural waste and resource recycling, and research on mechanized harvesting technology for cotton stalks has become one of the focuses of research on the whole mechanization technology of cotton production [5–8].

Cotton planting in foreign countries mainly adopts a large single-row standardized model. Most of the cotton stalk harvesting machinery is mainly based on the roller-type pulling machine, where Australia's MUTI harvester and the United States' AMADAS harvester are representative machines, which is difficult to adapt to the row spacing of machine cotton picking operations [9]. The cotton straw harvesters that have been developed in China mainly include the toothed-chain type [10], the toothed-disc type [11], the wallet type [12], and the clamping roller type [13]. Zhang et al. [10] developed the toothed-chain cotton straw harvester, which easily causes cotton straw blockage in the process of pulling cotton straw. Chen et al. [11,14] and Zhang Jiayi et al. [15] designed the toothed-disc cotton straw harvester, which easily clips or interrupts the cotton straw, increasing the breakage rate, and is not suitable for the dense planting mode in Xinjiang. Zhang Jiayi's team [12] designed a clip-type cotton straw harvester, which has high requirements for tensioning; insufficient tension of the belt will cause the phenomenon of cotton stalks being left behind, and the friction between the flexible materials generates significant heat. Tang et al. [16] developed the toothed-roller cotton straw harvester, which is wound with plastic film during operation, causing the machine to become stuck easily, and the performance of the machine is unstable, which increases energy consumption. Xie Jianhua's [13] team designed a clamping roller cotton stalk pulling machine, which requires a large bending angle of cotton straw and presents poor adaptability to cotton straw with low moisture content. There is little precipitation in Xinjiang, agriculture mainly depends on irrigation, and cotton planting has been mechanized, with tractors entering and exiting cotton fields to carry out operations many times, which leads to significant soil compaction in cotton fields after cotton harvest; if only the above-mentioned pulling mode is adopted, it easily causes cotton stalks to break, resulting in high breaking rates [9].

In order to solve the above problems, according to the soil conditions and the cotton planting model of one film and six rows in the Xinjiang cotton area, the root–soil complex model of cotton plants was established based on discrete elements; among them, the soil is represented by discrete element particles, and the root model was formed by bonding the discrete element particles with a suitable contact mechanics model [17,18]. The relationship among cotton roots, soil and a V-shaped root-cutting knife in the process of shoveling was studied by force analysis and simulation in the root-breaking process, and, finally, the parameters of the V-shaped root-cutting knife were optimized to determine its optimal design values to improve the pull-out rate of cotton straw [19,20].

## 2. Materials and Methods

### 2.1. Soil-Loosening and Root-Cutting Cotton Stalk Pulling and Gathering Machine

#### 2.1.1. The Structure and Working Principle of the Whole Machine

The soil-loosening and root-cutting cotton stalk pulling and gathering machine is mainly composed of a V-shaped root-cutting knife, a gathering device, a pulling device, and helicoid strips, as shown in Figure 1. The V-shaped root-cutting knife is installed behind the gathering device, the pulling device is located above the gathering device, and the helicoid strips are located behind the gathering device. The soil-loosening and root-cutting cotton stalk pulling and gathering machine needs to be pulled by a tractor to work. The V-shaped root-cutting knife cuts the root–soil complex of the cotton plant, shovels the cotton root, and loosens the soil. Hydraulic motor I drives the pulling device to rotate at high speed, and after root cutting, the cotton stalk is pulled and transported orderly to the helicoid strips. Hydraulic motor II drives the helicoid strips to rotate and complete the cotton stalk set-bar operation.

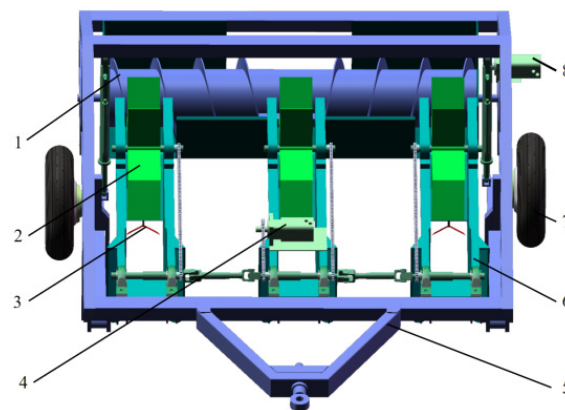


**Figure 1.** Structural diagram of soil-loosening and root-cutting cotton stalk pulling and gathering machine: 1. Helicoid strips; 2. pulling device; 3. V-shaped root-cutting knife; 4. hydraulic motor I; 5. traction frame; 6. gathering device; 7. walking wheel; 8. hydraulic motor II.

### 2.1.2. Technical Parameter

According to cotton planting patterns in Xinjiang [9], the main parameters of the soil-loosening and root-cutting cotton stalk pulling and gathering machine were determined, as shown in Table 1.

**Table 1.** The main parameters of the soil-loosening and root-cutting cotton stalk pulling and gathering machine.

Parameter	Values
Overall dimensions (length × width × height)/mm × mm × mm	2570 × 2230 × 1400
Working width/mm	2000
Width of V-shaped root-cutting knife/mm	6
Thickness of V-shaped root-cutting knife/mm	6
Operating width of single V-shaped root-cutting knife/mm	150
Width of gathering device/mm	150
Operating speed/m s <sup>-1</sup>	1.5
Reel wheel speed/r min <sup>-1</sup>	80
Helicoid strips speed/r min <sup>-1</sup>	140

## 2.2. Calculation of Key Parameters of the V-Shaped Root-Cutting Knife

### 2.2.1. Design of Slide Cutting Angle of the V-Shaped Root-Cutting Knife

The root-breaking operations are carried out by exerting cutting force on cotton roots through the V-shaped root-cutting knife, and the appropriate cutting force strength is an important guarantee to improve the pull-out rates of cotton stalks [21]. The slide cutting method can effectively reduce the cutting resistance and improve the cutting strength. Based on the sliding cutting principle, the V-shaped root-cutting knife with a slide cutting angle of  $\theta$  was designed to facilitate the slide cutting effect of the blade on cotton stalks and soil and improve the root-breaking rates of cotton stalks [22].

During sliding cutting, the forward speed  $V$  of the machine deviates from the normal direction of the blade, and the angle between the forward speed  $V$  of the machine and the normal direction is the slide cutting angle  $\theta$ . The slide cutting angle  $\theta$  reduces the actual wedge angle  $Y$  of the blade cutting into the material. A smaller slide cutting angle  $\theta$  makes the sliding cutting effect not obvious, but a larger slide cutting angle  $\theta$  will cause the blade to be very long, increase the surface friction between the V-shaped root-cutting knife and the soil, aggravate the wear of the blade, and increase the cutting resistance. The slide cutting angle is more suitable in a range of 20~55° [22]. Based on this, in order to obtain the ideal slide cutting angle of the V-shaped root-cutting knife, the critical condition of slide cutting was solved by establishing the kinematics and dynamics model of root breaking. Taking the forward direction of the knife as the  $y$ -axis, the plane rectangular

coordinate system was established on the cutting plane of the knife, as shown in Figure 2. Under the traction of the tractor, the V-shaped root-cutting knife performed root cutting operations along the  $y$ -axis direction, the contact point between a cotton root and the blade was regarded as a particle A, and the particle dynamics differential equation of the particle A along the tangential direction and the normal direction of the blade is

$$\begin{cases} F_n - F_t \cos \theta = ma_y \cos \theta \\ F_t \sin \theta - F_d = m(a_h - a_y \sin \theta) \end{cases} \quad (1)$$

where  $F_n$  is the normal force of the blade to particle, N;  $F_t$  is the friction force of root–soil complex on sliding particle A along  $Y$  axis, N;  $\theta$  is the slide cutting angle, °;  $m$  is the quality of slide cutting particle A, kg;  $a_y$  is the transport acceleration along the  $Y$ -axis direction,  $m/s^2$ ;  $F_d$  is the friction force of sliding cutting particle along the tangential direction of blade of the knife, N;  $a_h$  is the acceleration of sliding cutting particle along the tangential direction of blade of the knife,  $m/s^2$ .

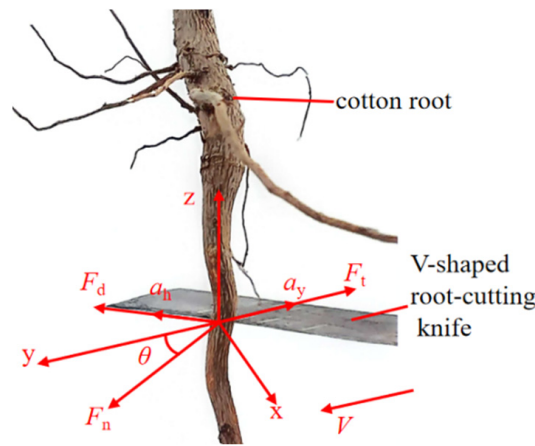


**Figure 2.** Analysis of slide cutting force of the V-shaped root-cutting knife.

The sliding cutting particle A had a tendency to move forward along the positive direction of the  $Y$ -axis during the cutting of the knife, while the root–soil complex had a friction force  $F_d$  along the negative direction of the  $Y$ -axis. If there is relative sliding between the knife and the sliding cutting particle A, there must be a relative movement trend between the two; therefore, the friction force  $F_d$  of the sliding cutting particle A along the tangential direction of the blade of the knife is

$$F_d = F_n f = F_n \tan \gamma \quad (2)$$

where  $f$  is the friction factor of sliding cutting particle and the blade of the knife;  $\gamma$  is the friction angle between sliding cutting particle and blade of the knife, °.

For (1) and (2), simultaneous simplification is available

$$F_n(\tan \theta - \tan \gamma) = ma_h \quad (3)$$

When the V-shaped root-cutting knife is used for root-cutting operation, to further reduce the cutting resistance, it is necessary to make the sliding cutting move between the particle A and the blade, that is,  $a_h > 0$ , and  $\gamma < \theta$  can be obtained from Formula (3). The friction angle between the sliding cutting particle and the blade is less than the slide cutting angle; at this time, the cotton roots not only bear the positive pressure of the blade but also bear the lateral force of the blade and slide along the edge direction during cutting. The friction angle between the cotton roots and the steel plate was measured by the slope sliding method, the friction angle between the cotton roots and the steel plate was  $35.9^\circ$ , and the designed slide cutting angle  $\theta$  of the blade should be greater than  $35.9^\circ$ .

### 2.2.2. Design of Cutting-Edge Angle of the V-Shaped Root-Cutting Knife

In order to sharpen the blade of the V-shaped root-cutting knife, optimize the cutting effect, reduce the working resistance, and improve the root cutting rates, it is necessary to cut the edge with a V-shaped root-cutting knife. The cutting-edge angle refers to the angle between the two cutting edges. The smaller the angle, the sharper the cutting edge, the smaller the resistance during cutting, and the more easily it cuts off the cotton root. However, too small a cutting-edge angle will make the cross-section area of the cutting edge too small, and the cutting-edge wear will be aggravated. The appropriate cutting-edge angle can not only ensure cutting performance but also reduce the operating resistance, reduce the knife wear, and improve the service life of the knife [23].

In order to obtain the optimal ranges of the cutting-edge knife of the V-shaped root-cutting knife, as shown in Figure 3, the resistance was analyzed, as shown in Formulas (4) and (5).

$$F_Z = 2\left(F_{A1} \cos \frac{\varphi}{2} + F_{A2} + F_{B1} \cos \frac{\varphi}{2} + F_{B2} + F_{C1} \sin \frac{\varphi}{2}\right) + F_f + C \quad (4)$$

$$F_{B1} = \mu F_{C1}$$

$$F_{B2} = \mu F_{C2} \quad (5)$$

$$F_C = P_i A_i$$

where  $F_z$  is the operating resistance of the V-shaped root-cutting knife, N;  $\varphi$  is the cutting-edge angle of the V-shaped root-cutting knife, °;  $F_{A1}$  is the soil adhesion force of the V-shaped root-cutting knife, N;  $F_{A2}$  is the soil adhesion force of the V-shaped root-cutting knife, N;  $F_{B1}$  is the soil friction of the V-shaped root-cutting knife, N;  $F_{B2}$  is the soil friction of the V-shaped root-cutting knife, N;  $F_{C1}$  is the normal force of soil on the V-shaped root-cutting knife, N;  $F_{C2}$  is the normal force of soil on the V-shaped root-cutting knife, N;  $C$  is the soil cohesion, N;  $F_f$  is the cutting resistance of cotton roots, N;  $\mu$  is the friction factor between soil and V-shaped root-cutting knife;  $P_i$  is the pressure on per unit area of the V-shaped root-cutting knife, Pa;  $A_i$  is the contact area between the V-shaped root-cutting knife and the soil, m;

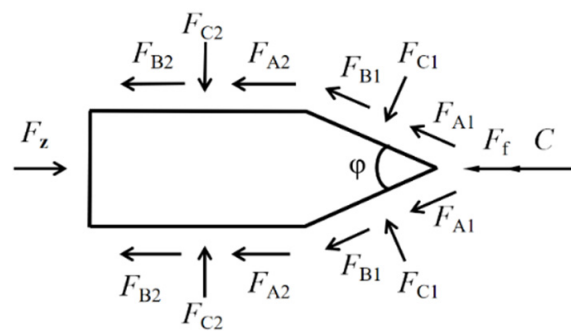


Figure 3. Shear force diagram of the V-shaped root-cutting knife.

From (4) and (5), we can obtain

$$F_Z = 2\left(F_{A2} \cos \frac{\varphi}{2} + F_{B1} + F_{B2}\right) + P_i A_i + \mu P_i A_i \cos \frac{\varphi}{2} + F_f + C \quad (6)$$

In order to obtain the minimum value of  $F_Z$ , the second derivative of (6) can be obtained.

$$\varphi = 2\arcsin \sqrt[3]{\frac{\mu P_i A_i}{F_{A2}}} \quad (7)$$

The sliding friction factor of soil and steel was measured by using the slope rolling method. The sliding friction factor of soil and steel was 0.192, and the tangential adhesion

force of soil was  $(2.6 \pm 1238)$  N [19,22]. Substituting it into Formula (7), the optimal ranges of the cutting-edge angle  $\varphi$  were  $43.18\sim 62.53^\circ$ .

### 2.2.3. Design of the Soil Entry Angle of the V-Shaped Root-Cutting Knife

Referring to the classification of tangent, the concept of the sliding cutting was elaborated in detail based on the angle between the surface of the V-shaped root-cutting knife and the direction of the cotton roots axis. The sliding cutting was divided into horizontal sliding cutting and oblique sliding cutting. Horizontal sliding cutting refers to the knife's surface being perpendicular to the cotton root axis and parallel to the direction of the knife movement. Oblique sliding cutting means that the knife surface is skewed to the cotton root axis and the direction of knife movement. Cellulose fiber is the main component of the plant cell wall, which endows cotton roots with strength and toughness. The direction of the cellulose fiber is approximately parallel to the cotton root axis. Therefore, when the cotton root is cut by two different sliding cutting methods, the angle between the direction of the V-shaped root-cutting knife cutting into the cotton root and the direction of the cotton root's own fiber is obviously different, and the cutting resistance and the root-cutting effect are also different. The angle between the surface of the V-shaped root-cutting knife and the normal line of the cotton root during the sliding cutting process is called the soil entry angle  $\beta$  [24]. When two different sliding cutting methods are used to cut the cotton roots, it is found that compared with the transverse sliding cutting, using the oblique sliding cutting has a better axial crushing effect on the cellulose; when the soil entry angle is  $13^\circ < \beta < 79^\circ$ , the cutting destructive force required for oblique sliding cutting can be reduced by 25.48~31.76% compared with horizontal sliding cutting, the cutting direction and the cutting surface of transverse sliding cutting are perpendicular to the axis of straw, and the anti-cutting strength of cotton root is the largest, so the cutting resistance of transverse sliding cutting is the largest. In order to reduce the area of the contact surface between the V-shaped root-cutting knife and the soil, the soil entry angle of the V-shaped root-cutting knife was designed to be  $13^\circ < \beta < 45^\circ$ .

### 2.3. Discrete Element Simulation of the V-Shaped Root-Cutting Knife

If field trials are used alone, it is difficult to observe the dynamic characteristics of cotton roots and soil particles from the microscopic point of view when studying the interaction of soil-touching components with the root–soil complex. At present, the combination of an experiment and numerical simulation is widely used [19,20]. The discrete element method has unique advantages in optimizing the parameters of the V-shaped root-cutting knife. The root–soil complex model constructed by using the discrete element method can simulate the relative displacement, rotation, friction, and collision between particles, so as to reflect the interaction between soil particles and cotton roots in the process of root breaking. The simulation results provided by the discrete element method can be processed and analyzed by visualization software to intuitively explain the source of cutting resistance and principle and effect of root cutting [17–19]. By simulating the cutting resistance and root-cutting effect of different parameter combinations of the V-shaped root-cutting knife, the influence of these parameters on the cutting resistance and root-cutting effect can be observed and analyzed. Using data analysis tools to statistically analyze the simulation results, the optimal combination of V-shaped root-cutting structure parameters can be quickly obtained, which can reduce the time and cost of actual tests and provide a scientific basis for the design of the V-shaped root-cutting knife parameters [18,22].

#### 2.3.1. Establishment of Discrete Element Interaction Model between the V-Shaped Root-Cutting Knife and Root–Soil Complex

Cotton is a typical Taproot crop, which is mainly composed of a main root deep into the soil, a small amount of lateral roots, and a large number of root hairs on the main roots and lateral roots. All roots are inverted and conical in the soil. In order to simplify the root–soil complex model and reduce the CPU calculation time to improve the simulation



efficiency [25], the cotton root model was simplified to a round table with an upper diameter of 13.84 mm, a lower diameter of 3.74 mm, and a height of 180 mm. In discrete elements, a six-cotton root model was established by using the rapid filling method with particles with a radius of 0.7 mm [26]. After completion, the time step was set as the initial time step, and an open-top soil trough with length, width, and height of 400 mm, 300 mm, and 200 mm was established. The particle factory was set up and filled with soil particles with a radius of 2 mm, and the filling time was 1 s. The research object selected in this study was the cotton area of Xinjiang, China. The significant soil compaction in the cotton fields by the cotton picker after cotton harvest, the adhesion force between soil and cotton root particles, and the adhesion force between soil particles and cotton roots are larger; therefore, the bond contact model (Hertz-Mindlin Bonding V2) was selected as the particle contact model [27], as shown in Figures 4 and 5. The addition time of Bonding V2 was set to 7 s in the Bond Creation Time of the particle factory. Based on the previous research work of this research group and the calibration of the parameters of the root–soil complex model by domestic and foreign scholars [28–30], the discrete element simulation parameters used in this study are shown in Table 2.

**Table 2.** Discrete element simulation parameters used in this study.

Parameter	Values	Parameter	Values
Density of soil/kg·m <sup>-3</sup>	2300	Coefficient of restitution of soil-soil	0.6
Poisson’s ratio of soil	0.35	Coefficient of static friction of soil-soil	0.45
Shear modulus of soil/MPa	1.07	Coefficient of rolling friction of soil-soil	0.21
Density of root/kg·m <sup>-3</sup>	825.8	Coefficient of restitution of root-root	0.384
Poisson’s ratio of root	0.35	Coefficient of static friction of root-root	0.597
Shear modulus of root/MPa	692	Coefficient of rolling friction of root-root	0.06
Density of shovel/kg·m <sup>-3</sup>	7865	Coefficient of restitution of root–soil	0.453
Poisson’s ratio of shovel	0.3	Coefficient of static friction of root–soil	0.625
Shear modulus of shovel/MPa	7.9 × 10 <sup>4</sup>	Coefficient of rolling friction of root–soil	0.7
Coefficient of restitution of soil-shovel	0.6	Coefficient of restitution of root-shovel	0.429
Coefficient of static friction of soil-shovel	0.6	Coefficient of static friction of root-shovel	0.561
Coefficient of rolling friction of soil-shovel	0.05	Coefficient of rolling friction of root-shovel	0.08
Normal Stiffness per it area of soil/N·m <sup>-3</sup>	5.302 × 10 <sup>8</sup>	Normal Stiffness per area of root/N·m <sup>-3</sup>	4.15 × 10 <sup>10</sup>
Shear Stiffness per uite area of soil/N·m <sup>-3</sup>	4.486 × 10 <sup>8</sup>	Shear Stiffness per unit area of root/N·m <sup>-3</sup>	5.6 × 10 <sup>10</sup>
Normal Strength of soil/Pa	5.5 × 10 <sup>5</sup>	Normal Strength of root/Pa	4 × 10 <sup>7</sup>
Shear Strength of soil/Pa	5.303 × 10 <sup>5</sup>	Shear Strength of root/Pa	5 × 10 <sup>7</sup>
Bonded Disk Scale of soil	2.4	Bonded Disk Scale of root	0.84

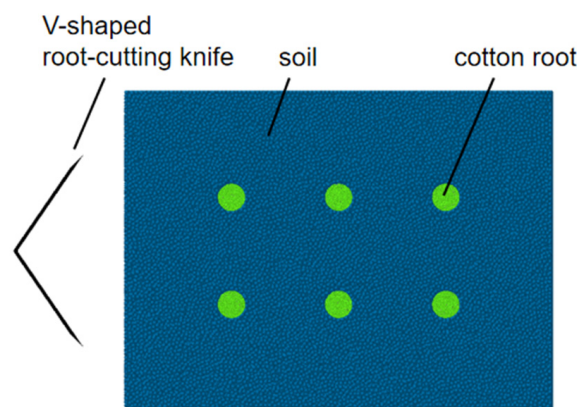


**Figure 4.** Vertical view of the discrete element model of the root–soil complex.

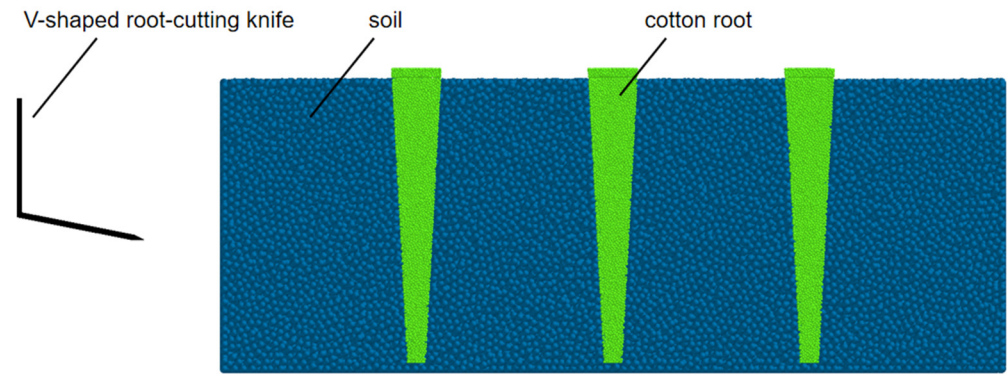


**Figure 5.** Main view of the discrete element model of the root–soil complex.

### 2.3.2. Simulated Tests

Through the above theory and simulation tests, it is found that the different slide cutting angle  $\theta$ , the cutting-edge angle  $\varphi$ , and the different soil entry angle  $\beta$  have significant effects on root cutting and cutting resistance. Therefore, the slide cutting angle  $\theta$ , the cutting-edge angle  $\varphi$ , and the soil entry angle  $\beta$  were selected as the test factors, and the three-factor and three-level orthogonal simulation test was carried out with the force required to cut the cotton roots (hereinafter referred to as the root-breaking force)  $Y_1$  and the mean value of the cutting resistance  $Y_2$  as the test indices. In the simulation process, according to the root morphology of cotton in the literature [25], the V-shaped root-cutting knife was selected to operate at a depth of 100 mm. The operating speed of cotton stalk harvesters in Xinjiang is 3~5 km·h<sup>-1</sup>. In this design, the operating speed of the soil-loosening and root-cutting cotton stalk pulling and gathering machine was set to 3.6 km·h<sup>-1</sup>. In order to make the simulation tests as practical as possible, the operating speed of the V-shaped root-cutting knife was set to 1 m·s<sup>-1</sup> in the simulation process, as shown in Figures 6–8. The factor coding for the response surface test is presented in Table 3.

**Table 3.** The factor coding for the response surface test.

Level	Slide Cutting Angle $X_1$ (°)	Cutting-Edge Angle $X_2$ (°)	Soil Entry Angle $X_3$ (°)
−1	36	43.2	13
0	45.5	53.35	29
1	55	63.5	45

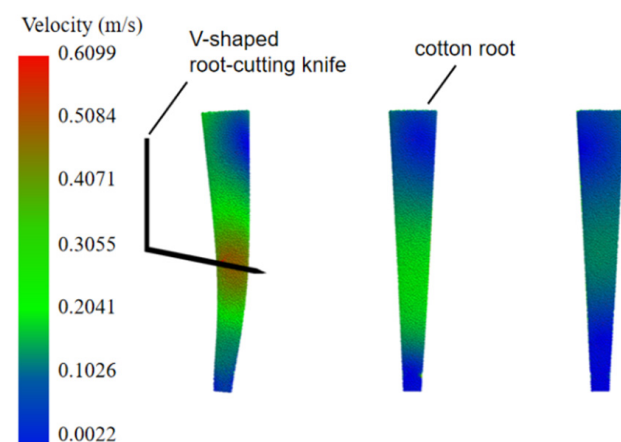


**Figure 6.** Root breaking contact diagram.



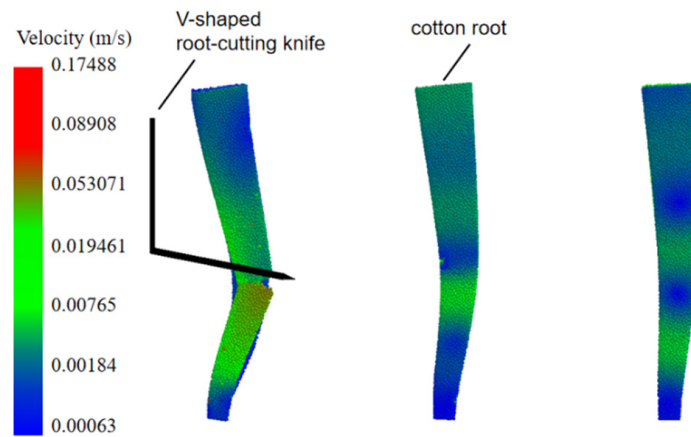


Figure 7. Root breaking instant picture.

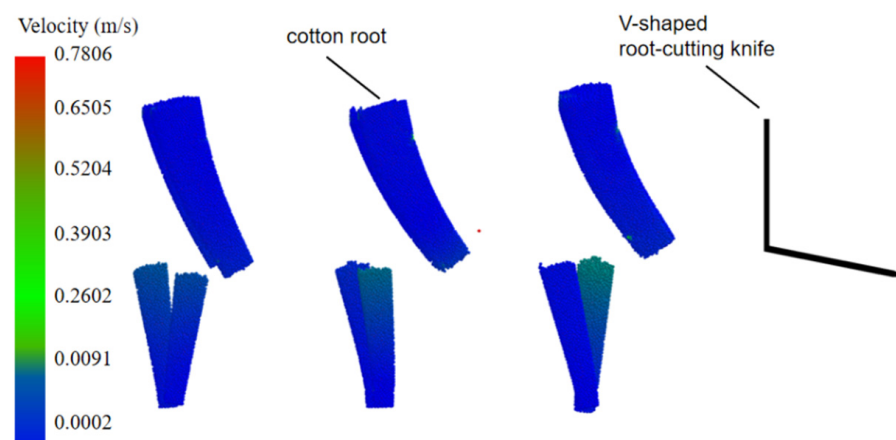


Figure 8. Completion diagram of root cutting.

According to the principle of the Box–Behnken experimental design, 17 sets of simulation experiments were carried out with the three-factor and three-level response surface analysis method, including 12 analysis factor experiments and 5 error experiments of zero-point estimation. The design and results of the response surface tests are shown in Table 4.

Table 4. The design and results of the response surface tests.

Test Number	X <sub>1</sub>	X <sub>2</sub>	X <sub>3</sub>	Root-Breaking Force	Mean Value of the Cutting Resistance
1	−1	0	−1	226.6	46.8
2	0	1	1	122.9	64.4
3	1	1	0	144.1	76.6
4	0	0	0	140.7	64.5
5	0	−1	1	98.6	70
6	1	0	1	108.2	78.7
7	0	1	−1	159.1	64
8	0	0	0	157.4	62.1
9	−1	1	0	195.1	50.2
10	0	0	0	140.2	62.1
11	1	0	−1	157.4	79.1
12	−1	−1	0	180.9	46.2
13	0	0	0	151.9	62.5
14	1	−1	0	82.5	77.2
15	−1	0	1	220.9	57.8
16	0	−1	−1	97.6	62
17	0	0	0	145.3	62.9

### 3. Simulation Results Analysis

#### 3.1. Analysis of Influencing Factors of the Root-Cutting Force and the Mean Value of Cutting Resistance of the V-Shaped Root-Cutting Knife

In Figure 9a–c, we show the change trend of the root-breaking force with an increase in the slide cutting angle, the cutting-edge angle, and the soil entry angle. In Figure 10a–c, the change trend of the mean value of the cutting resistance with an increase in the slide cutting angle, the cutting-edge angle, and the soil entry angle is presented. As shown in Figure 9a, with an increase in the slide cutting angle, the root-breaking force generally shows a downward trend, and the rate of decline is relatively rapid, particularly between  $36^\circ$  and  $45.5^\circ$ , while it slows down slightly between  $45.5^\circ$  and  $55^\circ$ . As shown in Figure 9b, with an increase in the cutting-edge angle, the root-breaking force generally shows an upward trend, and the rising speed is relatively fast, especially between  $36^\circ$  and  $45.5^\circ$ , and tends to be gentle between  $45.5^\circ$  and  $55^\circ$ . As shown in Figure 9c, with an increase in the soil entry angle, the root-breaking force generally presents a downward trend, and the rate of decline is relatively slow. As shown in Figure 10a, with an increase in the slide cutting angle, the mean value of the cutting resistance generally shows an upward trend, and the rising speed is relatively fast. As shown in Figure 10b, with an increase in the cutting-edge angle, the mean value of the cutting resistance generally shows an upward trend, and the rising speed is relatively slow. As shown in Figure 10c, with an increase in the soil entry angle, the mean value of the cutting resistance generally shows an upward trend, and the rising speed is relatively slow, especially between  $45.5^\circ$  and  $55^\circ$ , and slightly faster between  $36^\circ$  and  $45.5^\circ$ .

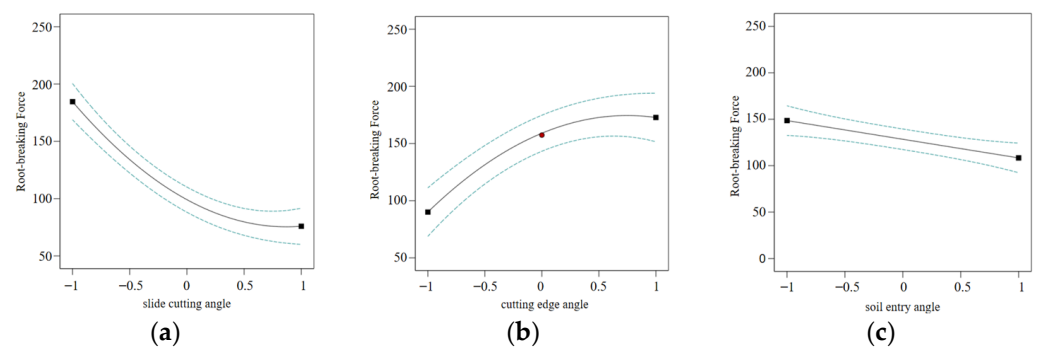


**Figure 9.** The change trend of the root-breaking force with an increase in the slide cutting angle, the cutting-edge angle, and the soil entry angle.

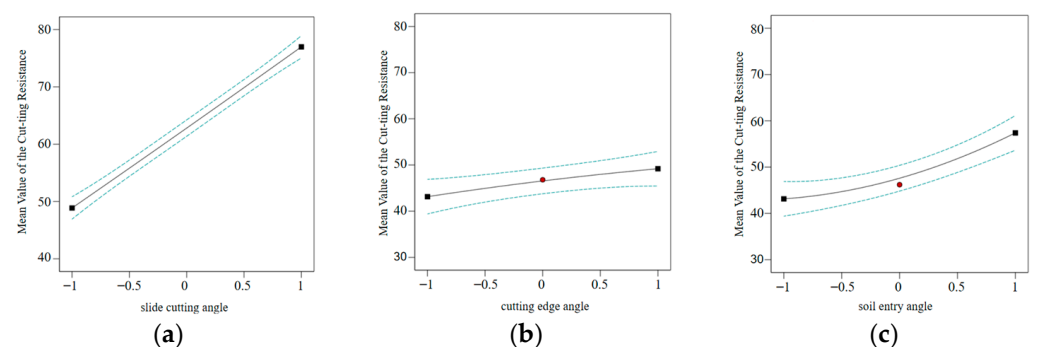


**Figure 10.** The change trend of the mean value of the cutting resistance with an increase in the slide cutting angle, the cutting-edge angle, and the soil entry angle.

The Design-Expert V13.0 software was used to analyze the variance properties of the regression equation. The variance analysis results of the root-breaking force and the mean value of the cutting resistance of the V-shaped root-cutting knife were obtained, as shown in Tables 5 and 6.

**Table 5.** Analysis of variance of the root-breaking force.

Source	Sum of Squares	df	Mean Square	F Value	p Value	Significant Degree
Model	26,305.24	9	2922.8	49.42	<0.0001	**
A	13,719.96	1	13,719.96	231.99	<0.0001	**
B	3264.32	1	3264.32	55.2	0.0001	**
C	1014.75	1	1014.75	17.16	0.0043	**
AB	561.69	1	561.69	9.5	0.0178	*
AC	473.06	1	473.06	8	0.0255	*
BC	345.96	1	345.96	5.85	0.0462	*
A <sup>2</sup>	4082.29	1	4082.29	69.03	<0.0001	**
B <sup>2</sup>	3204.51	1	3204.51	54.18	0.0002	**
C <sup>2</sup>	0.0059	1	0.0059	0.0001	0.9923	/
Residual	413.98	7	59.14			
Lack of Fit	193.04	3	64.35	1.16	0.4267	/
Pure Error	220.94	4	55.24			
Cor Total	26,719.22	16				

Note: “\*\*\*” indicates that the value is highly significant; \* indicates that the value is significant; / indicates that the value is not significant.

**Table 6.** Analysis of variance of the mean value of the cutting resistance.

Source	Sum of Squares	df	Mean Square	F Value	p Value	Significant Degree
Model	1656.8	9	184.09	99.87	<0.0001	**
A	1529.05	1	1529.05	829.52	<0.0001	**
B	0.005	1	0.005	0.0027	0.9599	/
C	45.13	1	45.13	24.48	0.0017	**
AB	5.29	1	5.29	2.87	0.1341	/
AC	32.49	1	32.49	17.63	0.0040	**
BC	14.44	1	14.44	7.83	0.0266	*
A <sup>2</sup>	0.0557	1	0.0557	0.0302	0.8669	/
B <sup>2</sup>	0.6241	1	0.6241	0.3386	0.5789	/
C <sup>2</sup>	29.9	1	29.9	16.22	0.0050	**
Residual	12.9	7	1.84			
Lack of Fit	8.94	3	2.98	3	0.1579	/
Pure Error	3.97	4	0.992			
Cor Total	1669.7	16				

Note: “\*\*\*” indicates that the value is highly significant; \* indicates that the value is significant; / indicates that the value is not significant.

Based on the analysis results in Tables 5 and 6, the  $p$  values of the  $Y_1$  regression model for the root-breaking force of the V-shaped root-cutting knife and the  $Y_2$  regression model for the mean value of the cutting resistance are both less than 0.0001, which indicates that the regression models are significant. The loss-of-fit term  $L$  was greater than 0.05 ( $L_{Y1} = 0.4267$ ,  $L_{Y2} = 0.1579$ , respectively), indicating that the regression equation had a high degree of fitting. The determination coefficients  $R_2$  of the equation are 0.9845 and 0.9923, indicating that this model can be used to explain more than 95% of the evaluation indices. It can be used to analyze and predict the root-breaking force  $Y_1$  and the mean value of the cutting resistance  $Y_2$  of the V-shaped root-cutting knife. It can be seen from Tables 5 and 6 that the slide cutting angle  $X_1$  and the soil entry angle  $X_3$  have a highly significant effect on  $Y_1$  and  $Y_2$  ( $p < 0.01$ ), and the cutting-edge angle  $X_2$  has a highly significant effect on  $Y_1$  ( $p < 0.01$ ). The significant factors influencing the root-breaking force in descending order were as follows: slide cutting angle  $\theta$ , cutting-edge angle  $\varphi$ , and soil entry angle  $\beta$ . The degrees of influence on the mean value of the cutting resistance were ordered as follows: slide cutting angle  $\theta$ , soil entry angle  $\beta$ , and cutting-edge angle  $\varphi$ .

### 3.2. Analysis of Response Surface Results

The response surface image can be used to analyze the interaction of the slide cutting angle  $\theta$ , the cutting-edge angle  $\varphi$ , and the soil entry angle  $\beta$  on the response values. Using the response surface software and combining the regression equations to analyze results, the response surface images were obtained, as shown in Figure 11. The interaction between the slide cutting angle  $\theta$  and the cutting-edge angle  $\varphi$  ( $X_1$   $X_2$ ), the interaction between the slide cutting angle  $\theta$  and the soil entry angle  $\beta$  ( $X_1$   $X_3$ ), and the interaction between the cutting-edge angle  $\varphi$  and the soil entry angle  $\beta$  ( $X_2$   $X_3$ ) had significant effects on the root-breaking force  $Y_1$  ( $p < 0.05$ ). The interaction between the slide cutting angle  $\theta$  and the soil entry angle  $\beta$  ( $X_1$   $X_3$ ) had a very significant effect on  $Y_2$  ( $p < 0.01$ ). The interaction between the cutting-edge angle  $\varphi$  and the soil entry angle  $\beta$  ( $X_2$   $X_3$ ) had a significant effect on the mean value of the cutting resistance  $Y_2$  ( $p < 0.05$ ).

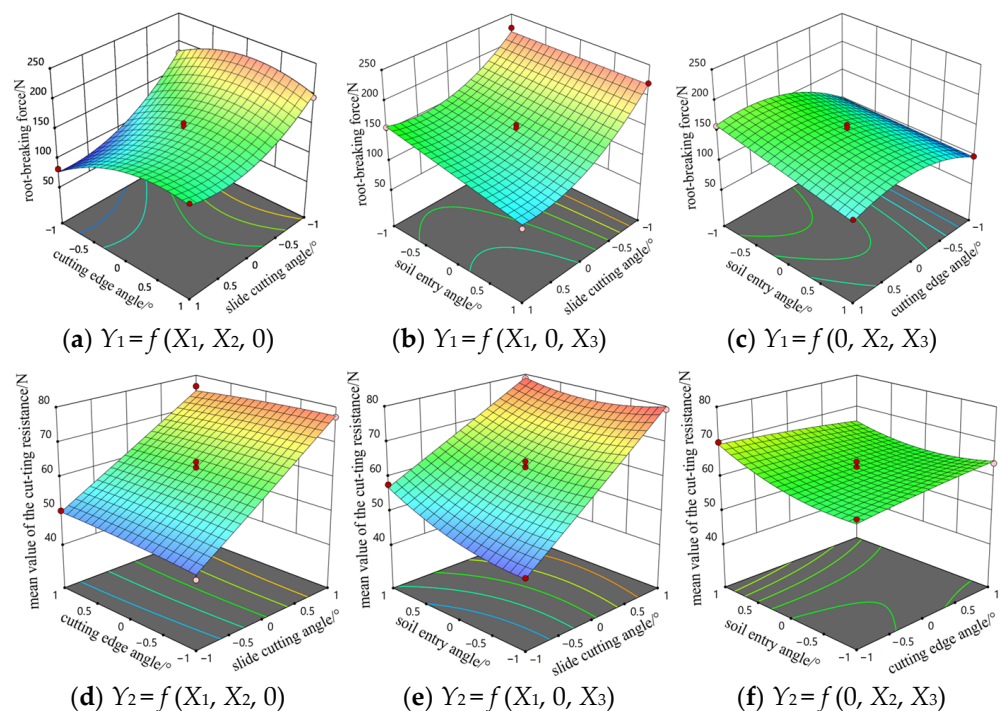


**Figure 11.** Response surface of the influence of experimental factor interaction on indicators.

From Figure 11, it can be seen that within the ranges of the experimental factors, when the cutting-edge angle  $X_2$  remains constant, the root-breaking force  $Y_1$  decreases as the slide cutting angle  $X_1$  and the soil entry angle  $X_3$  increase. This is because when the slide cutting angle and the soil entry angle become larger, the interaction between them leads to a smaller actual wedge angle  $Y$  of the cutting edge into the cotton roots, and the oblique sliding effect is more obvious. Therefore, the smaller the force required for the V-shaped root-cutting knife to cut the cotton roots, the more the mean value of the cutting resistance  $Y_2$  increases as the slide cutting angle  $X_1$  and the soil entry angle  $X_3$  increase. This is because when the slide cutting angle and the soil entry angle are larger, the interaction between the two leads to increases in the contact area between the V-shaped root-cutting knife and the soil, and, thus, the cutting resistance increases. When the slide cutting angle  $X_1$  remains constant, as the cutting-edge angle  $X_2$  and the soil entry angle  $X_3$  increase, the root-breaking force  $Y_1$  initially rises and then drops. This is because the smaller the cutting-edge angle, the sharper the cutting-edge angle, the larger the soil entry angle, the more distinct the oblique sliding effect, and the smaller the resistance during cutting. As the cutting-edge angle  $X_2$  and the soil entry angle  $X_3$  increase, the mean value of the cutting resistance  $Y_2$  rises, indicating that in comparison with the cutting-edge angle  $X_2$ , the soil entry angle  $X_3$  has a more significant effect on the mean value of the cutting resistance.

$Y_2$ . When the soil entry angle  $X_3$  remains constant, as the slide cutting angle  $X_1$  and the cutting-edge angle  $X_2$  increase, the interaction between the two decreases the root-breaking force  $Y_1$ , which indicates that the slide cutting angle  $X_1$  has a more significant influence on the root-breaking force  $Y_1$  than the cutting-edge angle  $X_2$ . The mean value of the cutting resistance  $Y_2$  rises as the slide cutting angle  $X_1$  and the cutting-edge angle  $X_2$  increase. This is because when the slide cutting angle and the cutting-edge angle are larger, the interaction between them increases the length of the blade, and the edge of the knife becomes dull; consequently, the cutting resistance increases.

### 3.3. Design of Optimized Parameters

The regression model equations regarding the influence of each factor on the root-breaking force  $Y_1$  and the mean value of the cutting resistance  $Y_2$  of the V-shaped root-cutting knife, after excluding insignificant factors, are presented in Equations (8) and (9).

$$Y_1 = 147.1 - 41.41X_1 + 20.2X_2 - 11.26X_3 + 11.85X_1X_2 - 10.88X_1X_3 - 9.3X_2X_3 + 31.14X_1^2 - 27.59X_2^2 \quad (8)$$

$$Y_2 = 62.82 + 13.83X_1 + 2.38X_3 - 2.85X_1X_3 - 1.9X_2X_3 + 2.67X_3^2 \quad (9)$$

$$\begin{cases} \min Y_1, \min Y_2 \\ \text{s.t.} \begin{cases} 36^\circ \leq X_1 \leq 55^\circ \\ 43.2^\circ \leq X_2 \leq 63.5^\circ \\ 13^\circ \leq X_3 \leq 45^\circ \end{cases} \end{cases} \quad (10)$$

The root-breaking force  $Y_1$  and mean value of the cutting resistance  $Y_2$  of the V-shaped root-cutting knife are important indices to evaluate the operating effect of the soil-loosening and root-cutting cotton stalk pulling and gathering machine. In order to find the optimal combination of operating parameters of the soil-loosening and root-cutting cotton stalks pulling and gathering machine and reduce the root-breaking rates and energy consumption of the machine, Design-Expert was used to optimize the root-breaking force and the mean value of the cutting resistance of the V-shaped root-cutting knife. The optimization range of the slide cutting angle of the V-shaped root-cutting knife was set between around 36 and 55°, the optimization range of the cutting-edge angle was set between around 43.2 and 63.5°, and the optimization range of the soil entry angle was set between around 13 and 45°. The optimization objectives were set as the minimum root-breaking force  $Y_1$  and the minimum mean value of the cutting resistance  $Y_2$  of the V-shaped root-cutting knife. The second optimization objective was equal weight (+ + +), and the optimization was carried out by means of experimental analysis software. According to the constraint conditions, the parameter combination optimization models were established, as shown in Equation (10).

The optimal test parameters were obtained as follows: the slide cutting angle of the V-shaped root-cutting knife is 48.3°, the cutting-edge angle is 43.4°, and the soil entry angle is 26.2°. At this time, the predicted root-breaking force of the V-shaped root-cutting knife is 87.15 N, and the predicted mean value of the cutting resistance is 63.39 N.

### 3.4. Field Test

To validate the optimized tests, we further optimized the optimal test coefficients. The V-shaped root-cutting knife was used with a slide cutting angle of 48.3°, a cutting-edge angle of 43.4°, and a soil entry angle of 26.2°. On 22 March 2024, the verification tests were carried out at the three consecutive test sites of the 145th Regiment in Shihezi City, Xinjiang. The soil firmness was 63.43 kPa, the soil moisture content was 10.46%, the cotton planting mode was one film and six rows, and the cotton variety was Xinluzao 84 (which is widely planted in Xinjiang and has the advantages of high yield and less disease). The operating speed of the soil-loosening and root-cutting cotton stalk pulling and gathering



machine was 1 m/s, and the operating depth was 100 mm. The main equipment used in the field tests is as follows: Kohl KE704B tractor (70 hp), soil-loosening and root-cutting cotton stalk pulling and gathering machine, soil firmness machine, soil moisture meter, ruler, tape, stopwatch, etc.

The tests were carried out with reference to GB/T 8097-2008 'Harvester Combine Test Method'. In order to ensure the stable operation of the tractor and reduce the errors, there was a 20 m stable area before the tractor entered the cotton stalks area to adjust the operating condition of the tractor. The length of the test area was 30 m, the tests were repeated three times, and the results of the tests were averaged. The test results are shown in Figure 12. The mean value of the pass rates for root breakage was 94.8%, and the mean value of pull-out rates of the cotton stalks was 93.2%.



**Figure 12.** Experiments of soil-loosening and root-cutting cotton stalk pulling and gathering machine.

### 3.5. The Calculation and Finite Element Analysis of the Minimum Specific Energy Consumption

The calculation formula of the specific energy consumption under the optimal parameters of the V-shaped root-cutting knife is shown in Formula (11).

$$E = \frac{W}{V} = \frac{FL}{V} \quad (11)$$

where  $E$  is the specific cutting energy consumption,  $\text{J}\cdot\text{m}^{-3}$ ;  $F$  is the mean value of the cutting resistance, N;  $L$  is the length of soil trough model, m;  $V$  is the volume of the soil trough model,  $\text{m}^3$ .

The minimum specific energy consumption of the V-shaped root-cutting knife is calculated to be  $41.26 \text{ J}\cdot\text{m}^{-3}$ .

In this research, the material of the V-shaped root-cutting knife is 45 # steel. Its shear modulus is  $7.9 \times 10^4 \text{ MPa}$ , the density is  $7865 \text{ kg}\cdot\text{m}^{-3}$ , the maximum yield strength is 355 MPa, and the Poisson's ratio is 0.3. Loads were exerted on all the stress surfaces of the V-shaped root-cutting knife to observe the overall stress and deformation. Figures 13 and 14 present a stress and deformation nephogram of the V-shaped root-cutting knife. As can be seen from the diagram, the stress of the V-shaped root-cutting knife is between approximately 0 and 4.01 MPa, which is far less than the yield strength of the V-shaped root-cutting knife, and the deformation is between 0 and 0.018 mm. The stress and deformation are small, which meets the use requirements.

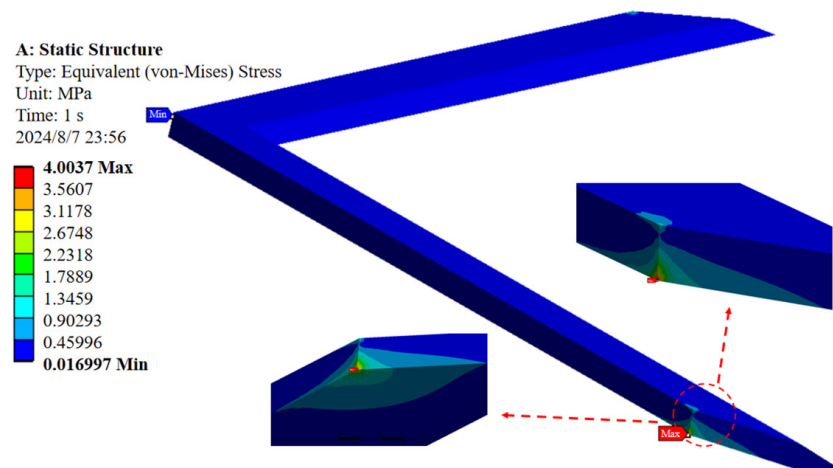


**Figure 13.** Equivalent (von-Mises) stress of the V-shaped root-cutting knife.

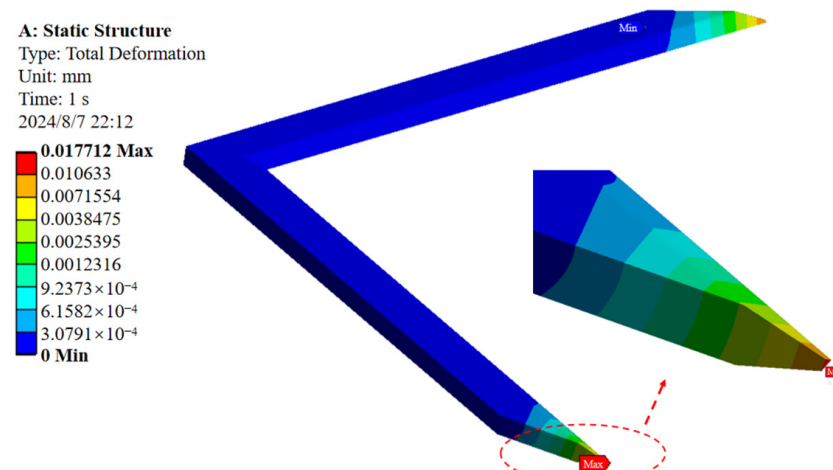


**Figure 14.** Total deformation of the V-shaped root-cutting knife.

#### 4. Conclusions

In order to solve the problems of the low reliability, high breakage rates, and high leakage rates of the existing pull-out devices, a soil-loosening and root-cutting cotton stalk pulling and gathering machine was designed. Through the kinematics and dynamics analysis of the root-cutting process, the main structural parameter ranges of the V-shaped root-cutting knife were obtained.

A simulation interaction model of the V-shaped root-cutting knife and the root–soil complex was established, taking the side cutting angle  $\theta$ , the cutting-edge angle  $\varphi$ , and the soil entry angle  $\beta$  of the V-shaped root-cutting knife as the test factors. The root-breaking force and the mean value of the cutting resistance were taken as the test indices to carry out the simulation tests. The test results show that the degrees of influence of each factor on the root-breaking force in a descending order were slide cutting angle  $\theta$ , cutting-edge angle  $\varphi$ , and soil entry angle  $\beta$ . The test results show that the degrees of influence of each factor on the mean value of the cutting resistance in a descending order were slide cutting angle  $\theta$ , soil entry angle  $\beta$ , and cutting-edge angle  $\varphi$ .

The established linear regression model was optimized, and the optimal combination of factors was obtained as follows: the slide cutting angle of the V-shaped root-cutting knife was 48.3°, the cutting-edge angle was 43.4°, and the soil entry angle was 26.2°. The field experiments were carried out with a forward speed of 1 m/s. The average pass rate of root-breaking was 94.8%, and the average pull-out rate of the cotton stalks was 93.2%, which proved the reliability of the optimized design of the V-shaped root-cutting knife.

This study can provide theoretical support for the design of a root-breaking cotton stalk pulling machine.

This study only analyzed the growth of the cotton roots under typical soil conditions (one-film and six-row planting mode) in the Xinjiang cotton area. Due to the limitation of experimental conditions, the influence of different soil environments on the cutting effect was not considered. Considering the analysis in this study, hardened soil does not easily remove cotton roots from; therefore, different soil conditions certainly have an impact on the root-cutting process of the V-shaped root-cutting knife. In the future, it will be necessary to analyze the different soil conditions and planting modes of cotton planting. By establishing a specific discrete element model of the root–soil complex, the optimal root-cutting parameters of the V-shaped root-cutting knife for different soil conditions were obtained.

**Author Contributions:** Resources, S.C.; data curation, Y.L.; writing—original draft preparation, H.L.; Software, H.L.; writing—review and editing, S.C. and H.M.; visualization, D.H.; supervision, S.C. and H.M.; project administration, S.C. and H.M.; formal analysis, L.H.; investigation, S.W.; validation, J.C. All authors have read and agreed to the published version of the manuscript.

**Funding:** This research was funded by the the National Key Research and Development Program of China (2022YFD2002400), the Autonomous Region Key research and development task special project of Xinjiang, China (2022B02033-2), the Bintuan Science and Technology Program (2023AB014), the Innovation Team of Xinjiang Academy of Agricultural and Reclamation Sciences (NCG202302) and Seventh Division—Shihezi University Science and Technology Innovation Special Project (QS2023006).

**Institutional Review Board Statement:** Not applicable.

**Data Availability Statement:** The data presented in this study are available on request from the corresponding authors.

**Acknowledgments:** The authors are grateful to the anonymous reviewers for their comments.

**Conflicts of Interest:** The authors declare no conflicts of interest.

## References

- Cheng, Y. Study on Fluctuation and Influencing Factors of Cotton Production in Xinjiang. Ph.D. Thesis, Shihezi University, Shihezi, China, 2022. (In Chinese)
- Sun, Z.Y. Research on the Adoption and Effectiveness Evaluation of Agricultural Socialized Services in Xinjiang Cotton Region. Ph.D. Thesis, Shihezi University, Shihezi, China, 2023. (In Chinese)
- Prakash, S.; Radha; Sharma, K.; Dhumal, S.; Senapathy, M.; Deshmukh, V.P.; Kumar, S.; Madhu; Anitha, T.; Balamurugan, V.; et al. Unlocking the potential of cottonstalk as a renewable source of cellulose: A review on advancements and emerging applications. *Int. J. Biol. Macromol.* **2024**, *261*, 129456. [[CrossRef](#)] [[PubMed](#)]
- Ding, X.H.; Yan, L.H.; Guo, C.; Jia, D.Z.; Guo, N.N.; Wang, L.X. Synergistic Effects between Lignin, Cellulose and Coal in the Co-Pyrolysis Process of coal and Cotton Stalk. *Molecules* **2023**, *28*, 5708. [[CrossRef](#)] [[PubMed](#)]
- Narendra, R.; Yang, Y.Q. Properties and potential applications of natural cellulose fibers from the bark of cotton stalks. *Bioresour. Technol.* **2009**, *100*, 3563–3569.
- Cai, C.G.; Wang, Z.B.; Ma, L.; Xu, Z.X.; Yu, J.M.; Li, F.G. Cotton stalk valorization towards bio-based materials, chemicals, and biofuels: A review. *Renew. Sustain. Energy Rev.* **2024**, *202*, 114651. [[CrossRef](#)]
- Dong, Z.; Hou, X.L.; Ian, H.; Yang, Y.Q. Preparation and properties of cotton stalk bark fibers and their cotton blended yarns and fabrics. *J. Clean. Prod.* **2016**, *139*, 267–276. [[CrossRef](#)]
- Li, H.; Zhao, C.S.; Han, W.J.; Jiang, Y.F.; Wang, S. Preparation and Research of Environment-friendly Degradable Paper Mulching Film of Cotton Stalk Fiber. *IOP Conf. Ser. Earth Environ. Sci.* **2018**, *199*, 042052. [[CrossRef](#)]
- Shen, C.J.; Guo, H.J.; Dai, Y.M.; Li, F.; Cao, S.L.; Jin, X.W.; Shen, L.; Deng, Y. Situation and strategies of mechanization in recycling of cotton stalk in Xinjiang. *J. Huazhong Agric. Univ.* **2023**, *42*, 53–63. (In Chinese)
- Zhang, J.X.; Wang, T.Y.; Chen, M.J.; Zhao, W.S.; Wang, Z.W.; Yeerbolatl, T.M.E.; Wang, Y.C.; Liu, X.; Liu, A.P. Design of toothed disc cotton stalk harvester. *Trans. Chin. Soc. Agric. Eng.* **2019**, *35*, 1–8. (In Chinese)
- Chen, M.J.; Zhao, W.S.; Wang, Z.W.; Liu, K.K.; Chen, Y.S.; Hu, Z.C. Operation Process Analysis and Parameter Optimization of Dentate Disc Cotton-stalk Uprooting Mechanism. *Trans. Chin. Soc. Agric. Mach.* **2019**, *50*, 109–120. (In Chinese)
- Zhang, J.X.; Rui, Z.Y.; Cai, J.L.; Wang, Y.C.; Yeerbolatl, T.M.E.; Gao, Z.M. Design and Test of Front Mounted Belt Clamping and Conveying Cotton-stalk Pulling Device. *Trans. Chin. Soc. Agric. Mach.* **2021**, *52*, 77–84. (In Chinese)

13. Xie, J.H.; Wu, S.H.; Cao, S.L.; Zhang, Y.; Zhao, W.S.; Zhou, J.B. Design and Experiment of Clamping Roller Cotton Stalk Extraction Device. *Trans. Chin. Soc. Agric. Mach.* **2023**, *54*, 101–111. (In Chinese)
14. Chen, M.J. Research on the Key Technology of Dentate Disc Cotton-stalk Uprooting Machine. Ph.D. Thesis, Chinese Academy of Agricultural Sciences, Beijing, China, 2022. (In Chinese)
15. Zhang, J.X.; Yang, R.; Wang, Z.W.; Hou, C.F.; Wang, Y.C.; Cai, J.L.; Yansenjiang, B.K.L.; Guo, G. Design and test of the cottonstalk pulling equipment with toothed plate. *Trans. Chin. Soc. Agric. Eng.* **2024**, *40*, 41–50. (In Chinese)
16. Tang, Z.F.; Han, Z.D.; Gan, B.X.; Bao, C.L.; Hao, F.P. Design and Experiment on Cotton Stalk Pulling Head with Regardless of Row. *Trans. Chin. Soc. Agric. Eng.* **2010**, *41*, 80–85. (In Chinese)
17. Chen, W.X.; Ren, J.B.; Huang, W.L.; Chen, L.B.; Weng, W.X.; Chen, C.C.; Zheng, S.H. Design and Parameter Optimization of a Dual-Disc Trenching Device for Ecological Tea Plantations. *Agriculture* **2024**, *14*, 704. [[CrossRef](#)]
18. Zhang, B.; Chen, J.; Zhu, Y.Y. Improved Design and Simulation of an Integrated Ridge-Breaking Earth Cultivator for Ratoon Sugarcane Fields. *Agriculture* **2024**, *14*, 1013. [[CrossRef](#)]
19. Awuah, E.; Zhou, J.; Liang, Z.; Aikins, K.A.; Gbenontin, B.V.; Mecha, P.; Makange, N.R. Parametric analysis and numerical optimisation of Jerusalem artichoke vibrating digging shovel using discrete element method. *Soil Tillage Res.* **2022**, *219*, 105344. [[CrossRef](#)]
20. Zhou, W.Q.; Ni, X.; Song, K.; Wen, N.; Wang, J.W.; Fu, Q.; Na, M.J.; Tang, H.; Wang, Q. Bionic Optimization Design and Discrete Element Experimental Design of Carrot Combine Harvester Ripping Shovel. *Processes* **2023**, *11*, 1526. [[CrossRef](#)]
21. Huang, W.T.; Zhao, D.; Liu, C.; Meng, X.J.; Kong, L.H.; Du, W.H. Optimization of garlic digging shovel parameters based on EDEM and quadratic regression orthogonal rotation combination design. In Proceedings of the 2020 3rd World Conference on Mechanical Engineering and Intelligent Manufacturing (WCMEIM), Shanghai, China, 4–6 December 2020; pp. 707–711.
22. Zou, L.L.; Yan, D.W.; Niu, Z.R.; Yuan, J.; Cheng, H.; Zheng, H. Parametric analysis and numerical optimisation of spinach root vibration shovel cutting using discrete element method. *Comput. Electron. Agric.* **2023**, *212*, 108138. [[CrossRef](#)]
23. Liu, S.H.; Weng, S.J.; Liao, Y.L.; Zhu, D.Y. Structural Bionic Design for Digging Shovel of cassava Harvester Considering Soil Mechanics. *Appl. Bionics Biomech.* **2014**, *11*, 1–2. [[CrossRef](#)]
24. Gao, J.M.; Jin, Z.P.; Ai, A.J. The Optimized Design of Soil-Touching Parts of a Greenhouse Humanoid Weeding Shovel Based on Strain Sensing and DEM-ADAMS Coupling simulation. *Sensors* **2024**, *24*, 868. [[CrossRef](#)]
25. Zhu, L.Y. Study on Cotton Root and Shoot Morphological and Physiological Characteristics and Root Transcriptome under Low Nitrogen Conditions. Ph.D. Thesis, Hebei Agricultural University, Baoding, China, 2022. (In Chinese)
26. Coetzee, C.J.; Lombard, C.J.; Coetzee, S.G.; Lombard, S.G. The destemming of grapes: Experiments and discrete element modelling. *Biosyst. Eng.* **2013**, *114*, 232–248. [[CrossRef](#)]
27. Luo, Q.; Huang, X.P.; Wu, J.F.; Mou, X.B.; Li, S.Y.; Ma, G.J.; Wan, F.X.; Peng, L.Z. Simulation Analysis and Parameter Optimization of Seed-Flesh Separation Process of Seed Melon Crushing and Seed Extraction Separator Based on DEM. *Agriculture* **2024**, *14*, 1008. [[CrossRef](#)]
28. Li, J.L.; Lu, Y.T.; Peng, X.B.; Jiang, P.; Zhang, B.C.; Zhang, L.Y.; Meng, H.W.; Kan, Z.; Wang, X.Z. Discrete element method for simulation and calibration of cotton stalk contact parameters. *BioResources* **2022**, *18*, 400–416. [[CrossRef](#)]
29. Zhang, J.X.; Zang, P.; Zhang, H.; Tan, C.L.; Wan, W.Y.; Wang, Y.C. Calibration of Simulation Parameters of Xinjiang Cotton Straw Based on Discrete Element Method. *Trans. Chin. Soc. Agric. Mach.* **2023**, *55*, 11–16. (In Chinese)
30. Jiang, D.L.; Chen, X.G.; Yan, L.M.; Gou, H.X.; Yang, J.C.; Li, Y. Parameter Calibration of Discrete Element Model for Cotton Rootstalk–Soil Mixture at Harvest Stage in Xinjiang Cotton Field. *Agriculture* **2023**, *13*, 1344. [[CrossRef](#)]

**Disclaimer/Publisher’s Note:** The statements, opinions and data contained in all publications are solely those of the individual author(s) and contributor(s) and not of MDPI and/or the editor(s). MDPI and/or the editor(s) disclaim responsibility for any injury to people or property resulting from any ideas, methods, instructions or products referred to in the content.